Heliyon 8 (2022) e09099

Contents lists available at ScienceDirect

Heliyon

journal homepage: www.cell.com/heliyon

Research article

Potential enhancement of metformin hydrochloride in solidified reverse micellar solution-based PEGylated lipid nanoparticles targeting therapeutic efficacy in diabetes treatment

Franklin Chimaobi Kenechukwu *, Daniel Okwudili Nnamani, Judith Chekwube Duhu, Bright Ugochukwu Nmesirionye, Mumuni Audu Momoh, Paul Achile Akpa, Anthony Amaechi Attama

Drug Delivery and Nanomedicines Research Group, Department of Pharmaceutics, Faculty of Pharmaceutical Sciences, University of Nigeria, Nsukka, 410001, Enugu State, Nigeria

ARTICLE INFO

Keywords:
PEGylated solid lipid nanoparticles
Solidified reverse micellar solution (SRMS)
Metformin
Beeswax
Anti-diabetic activity
Phospholipon ® 90H

ABSTRACT

Metformin hydrochloride (MH) is a widely used oral biguanide antihyperglycemic (antidiabetic) drug with poor bioavailability which necessitates the development of novel drug delivery systems such as PEGylated solid lipid nanoparticles for improving its therapeutic activity. The aim of this study was to formulate, characterize and evaluate *in vitro* and *in vivo* pharmacodynamic properties of metformin–loaded PEGylated solid lipid nanoparticles (PEG-SLN) for improved delivery of MH. The lipid matrices (non-PEGylated lipid matrix and PEGylated lipid matrices) used in the formulation of both non-PEGylated (J_0) and PEGylated SLNs (J_{10}, J_{20}, J_{40}) were prepared by fusion using beeswax and Phospholipon ® 90H at 7:3 ratio with or without polyethylene glycol (PEG) 4000 (0, 10, 20 and 40% w/w), respectively. Representative lipid matrices (LM and PEG-LM) were loaded with MH by fusion and then characterized by differential scanning calorimetry (DSC) and Fourier transform infrared (FT-IR) spectroscopy. The PEG-SLNs were prepared by high shear hot homogenization using the lipid matrices (5% w/w), drug (MH) (1.0% w/w), sorbitol (4% w/w) (cryoprotectant), Tween ® 80 (2% w/w) (surfactant) and distilled water (q.s to 100% w/w) (vehicle). The non-PEGylated and PEGylated SLNs (J_0, J_{10}, J_{20}, J_{40})) were characterized with respect to encapsulation efficiency (EE%), loading capacity (LC), morphology by scanning electron microscopy (SEM), mean particle size (Z_{av}) and polydispersity indices (PDI) by photon correlation spectroscopy (PCS), compatibility by FT-IR spectroscopy and *in vitro* drug release in biorelevant medium. Thereafter, *in vivo* antidiabetic study was carried out in alloxanized rats' model and compared with controls (pure sample of MH and commercial MH- Glucophage®)). Solid state characterizations indicated the amorphous nature of MH in the drug loaded-lipid matrices. The PEG-SLNs were mostly smooth and spherical nanoformulations with Z_{av} and PDI of 350.00 nm and 0.54, respectively, for non-PEGylated SLNs, and in the range of 386.80–783.10 nm and 0.592 to 0.752, respectively, for PEGylated SLNs. The highest EE% and LC were noted in batch J_{20} and were 99.28% and 16.57, respectively. There was no strong chemical interaction between the drug and excipients used in the preparation of the formulations. The PEGylated SLN (batch J_{40}) exhibited the highest percentage drug released (60%) at 8 h. The PEGylated SLNs showed greater hyperglycemic control than the marketed formulation (Glucophage ®) after 24 h. This study has shown that metformin–loaded PEGylated solid lipid nanoparticles could be employed as a potential approach to improve the delivery of MH in oral diabetic management, thus encouraging further development of the formulations.

1. Introduction

Diabetes is a group of metabolic diseases characterized by hyperglycaemia resulting from defects in insulin secretion, insulin action, or both [1]. The resultant hyperglycaemia produces severe complications and the classical symptoms of polyuria, polydipsia and polyphagia [2]. Diabetes is one of the leading causes of mortality, posing a huge challenge to the global community due to its escalating cost of management.

* Corresponding author.
E-mail addresses: frankline.kenechukwu@unn.edu.ng, chimafrankduff@yahoo.com, kenechukwufc.cnpq-twaspostdoc@ima.ufrj.br (F.C. Kenechukwu).

https://doi.org/10.1016/j.heliyon.2022.e09099
Received 2 July 2021; Received in revised form 9 November 2021; Accepted 9 March 2022

Table 1. Formulation composition of lipid matrices for PEGylated and non-PEGylated SLNs preparation.

Sample	Ingredients (%w/w)
LM (7:3)	Beeswax (70) and Phospholipon® 90H (30)
PEG-LM (0:10)	PEG 4000 (0) and LM (100)
PEG-LM (1:9)	PEG 4000 10 and LM (90)
PEG-LM (2:8)	PEG 4000 (20) and LM (80)
PEG-LM (4:6)	PEG 4000 (40) and LM (60)59

Table 2. Optimized formula for the preparation of the non-PEGylated and PEGylated SLNs.

Lipid matrix		5.0% w/w
Metformin		1.0% w/w
Polysorbate® 80 (Tween® 80)		2.0% w/w
Sorbitol		4.0% w/w
Water	q.s. to	100% w/w

According to the International Diabetes Federation (IDF) atlas 2019 update, about 463 million adults (20–79 years) worldwide are living with diabetes and this is projected to rise to 700 million (51%) by 2045 [3], majority of those living with diabetes, lives in low-and middle-income countries. In Africa, about 19 million are living with diabetes with a prevalence rate of 3.9%. This however, is projected to increase by 143.3% by 2045 [3]. This region also accounts for the highest proportion of undiagnosed diabetes, with most of the populace unaware of their condition. Worthy of note is that both the number of cases and the prevalence of diabetes have been steadily increasing over the past few decades. Diabetes accounts for 6.8 % of mortality rate in Africa, with an annual expenditure of 9.5 billion USD on diabetes-related health expenditure [3]. For a disorder that has been extensively researched on, with an armamentarium of drugs, such prevalence, number of cases and mortality are highly undesirable and worrisome.

Biguanides are one of the classes of drugs used in the management of diabetes. Metformin is the only available biguanide. It is the most popular oral glucose-lowering medication, widely viewed as 'foundation therapy' for individuals with newly diagnosed type 2 diabetes mellitus [4]. Metformin acts by increasing insulin sensitivity and decreasing gluconeogenesis. Metformin belongs to class III drugs in the biopharmaceutical classification system (BCS), drugs in this class are characterized by low permeability and high solubility. Metformin's widespread use is however plagued by a plethora of problems and undesirable side effects that limits its therapeutic efficiency including low bioavailability, high dose, frequent dosage, gastrointestinal side effects and poor intestinal absorption due to the cationic biguanide structure, thus the transmembrane transport of metformin is highly dependent on the organic cation transporter (OCTs) [5, 6, 7, 8]. In order to surmount these problems and side effects associated with metformin use, several formulation techniques have been utilized to deliver metformin however most of this

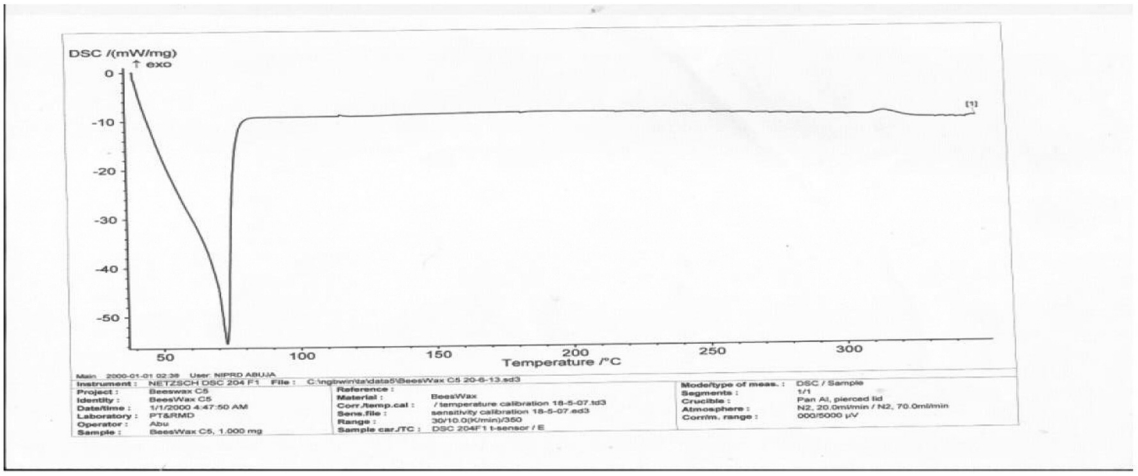

Figure 1. Differential scanning calorimetry (DSC) thermogram of beeswax (BW).

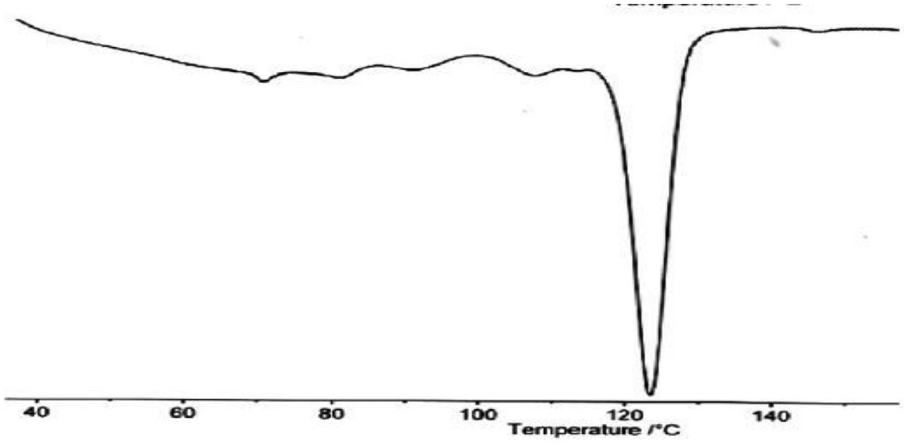

Figure 2. Differential scanning calorimetry (DSC) thermogram of Phospholipon® 90H (P90H).

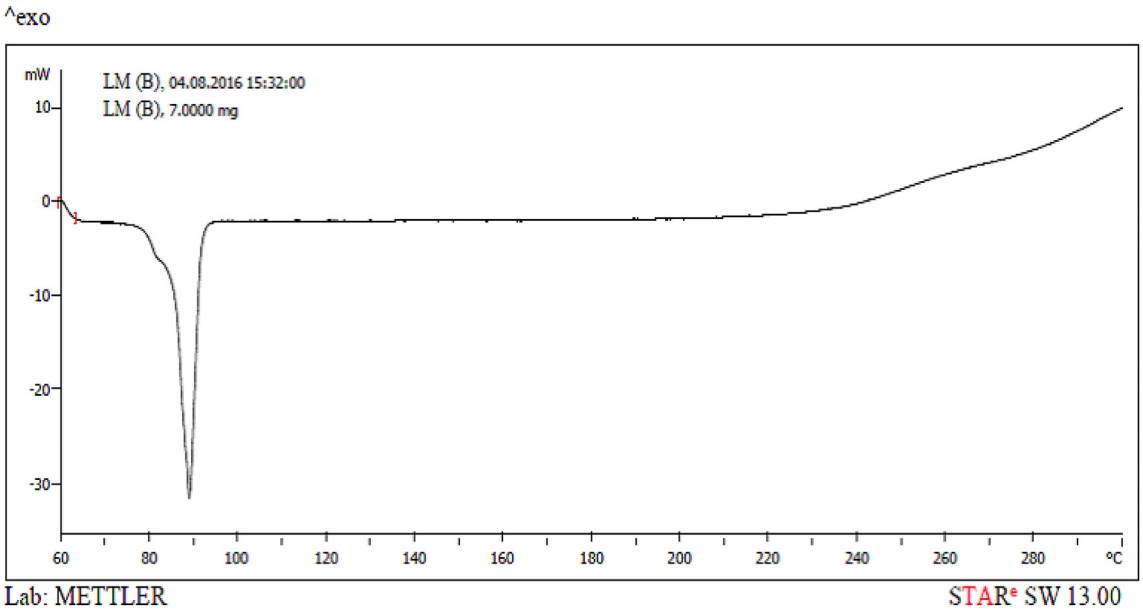

Figure 3. Differential scanning calorimetry (DSC) thermogram of structured lipid matrix (BW: P90H) (7:3) (LM_1).

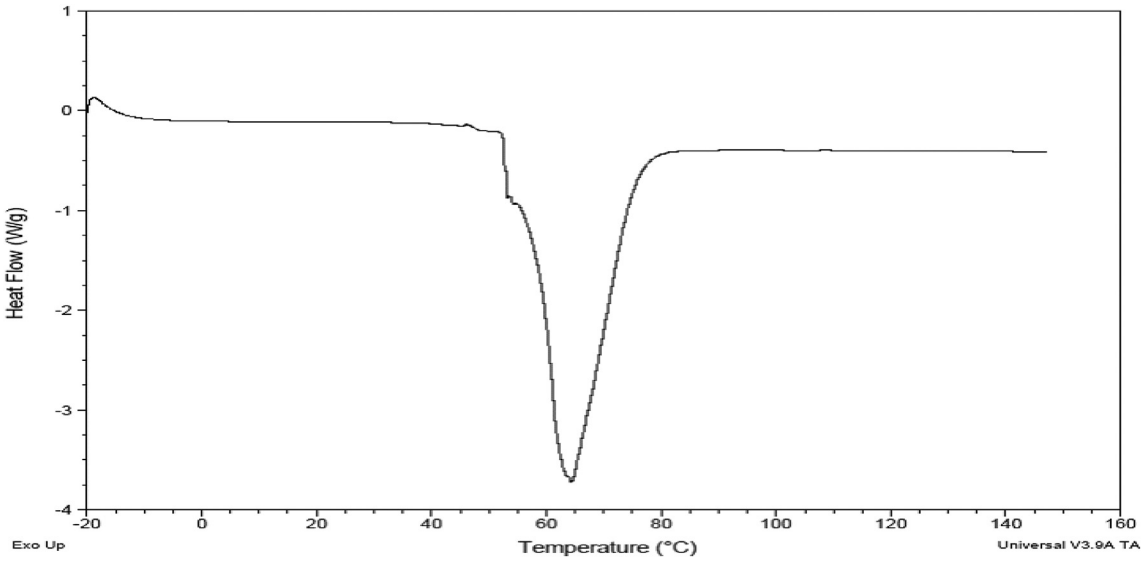

Figure 4. Differential scanning calorimetry (DSC) thermogram of PEG 4000.

formulation strategies demonstrated varying degrees of failures hence the need to brainstorm for more efficient method of delivering this drug. Recent advances in nanotechnology and nanoparticulate systems for improved drug delivery shows great potential for the administration of wide variety of active pharmaceuticals [9].

Several attempts have been made to enhance the oral delivery of metformin; some of which includes liposomes [10], PEGylated-mucin for oral delivery [11], alginate nanoparticles [12], hyaluronic acid nanoparticles [13], chitosan nanoparticles [14], chitosan/eudragit nanocomplex [15], niosomes [16], topical gel for dermal delivery [17], solid lipid microparticles [5], solid lipid nanoparticle for transdermal delivery [18]. Some other lipid-based drug delivery systems include lipid drug conjugates (LDC), solid lipid nanoparticles (SLN), nanostructured lipid carrier (NLC). Lipid nanoparticles's extensive use in drug delivery systems is due to the fact that lipid matrices are safe, biocompatible, non-toxic, easily manufactured industrially and versatile rendering it to be suitable for different routes of administration marking the pre-requisites for any ideal drug delivery vehicle [19, 20, 21]. Solid lipid nanoparticles (SLNs) developed in the early 1990s as alternative delivery systems to liposomes, emulsions, and polymeric nanoparticles [22, 23, 24], are at the forefront of the rapidly developing field of nanotechnology with several potential applications in drug delivery, clinical medicine, and research [25]. They are mainly composed of solid lipids (with melting point above 40 °C), surfactant (stabilizer), co-surfactant (water/solvent) and active ingredients [26,27] with mean particle size within the submicron range typically ranging between 50-1000 nm [28], and lipid concentration varying from 0.1% to 30% and surfactant concentration from 0.5 to 5% [19]. This minuscule size of SLNs permits them

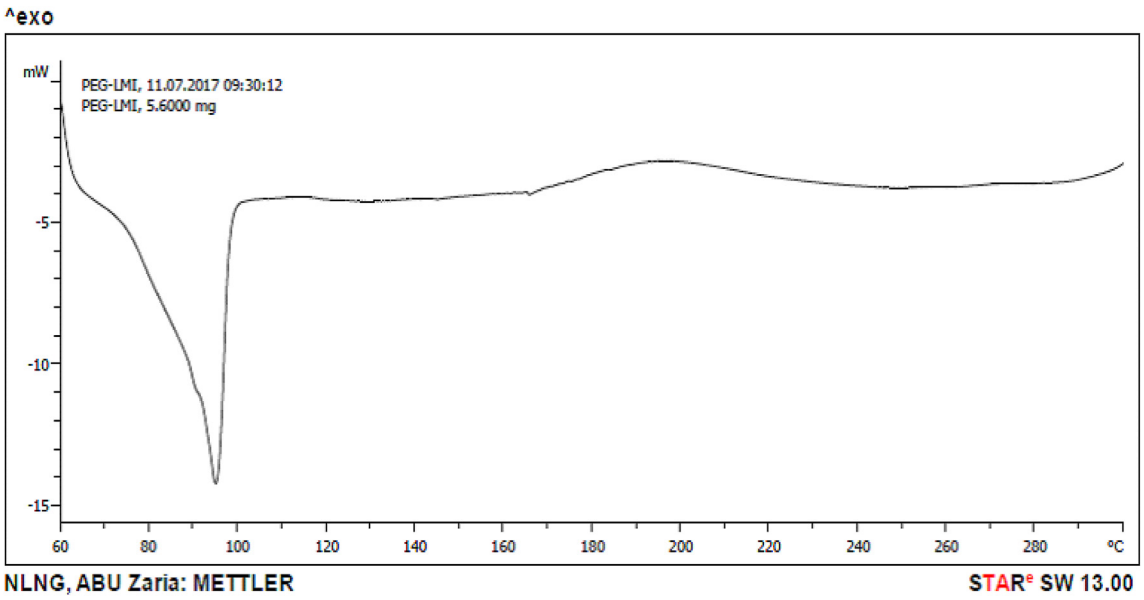

Figure 5. Differential scanning calorimetry (DSC) thermogram of PEGylated lipid matrix (PEG-LM_1).

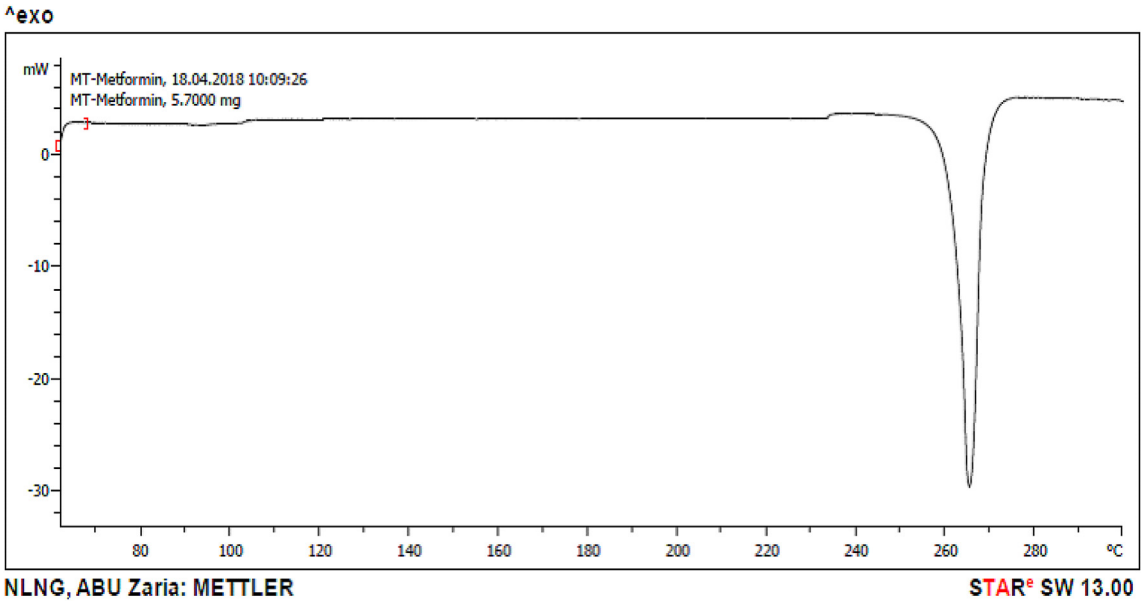

Figure 6. Differential scanning calorimetry (DSC) thermogram of metformin.

to cross tight endothelial cells and escape from the reticuloendothelial system (RES) thus bypassing the liver and spleen filtration [29,30]. SLNs have high drug entrapment capability and the drugs entrapped within its lipid matrix is stable. Since the lipids used in SLN formulations have melting points above that the human body temperature, the solid lipid nanoparticles remain as solids after administration, they give a prolonged released of the drug over time.

PEGylation is one of the most promising and extensively studied strategies for improving the performance of drugs and bioactives, it is mainly characterized by the use of very small quantities of substance for therapy [31]. Modifying nanoparticles by PEGylation can significantly change drug metabolic process in blood by protecting it from metabolism [32, 33, 34]. The use of polyethylene glycol (PEG) in nano formulations imparts stealth properties on the nanoparticles [35], reduces the tendency of elimination by the reticuloendothelial system (RES), improves the bioavailability and half-life of drug used in the formulation [36]. PEG is hydrophilic thus its hydrophilic properties could prevent interaction with other nanoparticles *via* sterical hindrance, thereby improving the stability of nanoparticles [37]. Claims also show that PEG enhances the mucoadhesive properties of nanoparticles [38], metformin being a class III drug in the BCS classification have high solubility and low permeability thus formulating it as a PEGylated lipid nanoparticle will help impart a lipophilic character to the hydrophilic metformin, this will help better membrane permeability [39] thereby increasing its bioavailability. This technique have been used to enhance the therapeutic efficacy of drugs by enabling increased drug concentration and longer dwelling time at the site of action [40,41]. Thus, PEGylation could be utilized in the enhancement of the delivery of metformin. The novelty embodied in this study is the use of PEGylated nanocarrier to enhance the antidiabetic activity of metformin via improved half-life, reduced dosage and dosing frequency as well as through enhanced permeability across the biological membrane.

Although PEGylated carriers of metformin have been developed by our research group [11,42], there is currently a dearth of information in

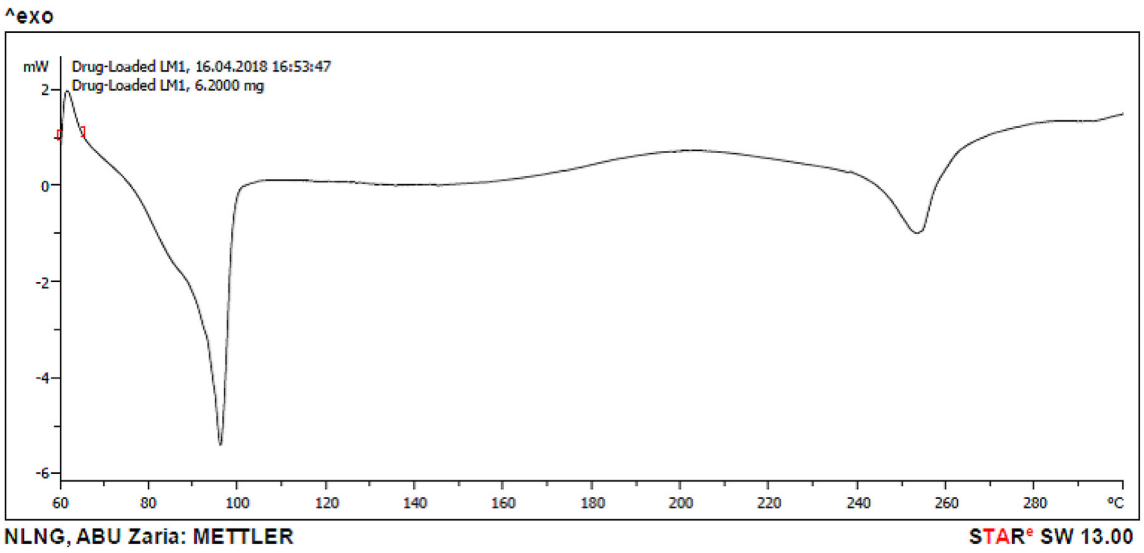

Figure 7. Differential scanning calorimetry (DSC) thermogram of metformin-loaded lipid matrix (Drug-loaded LM_1).

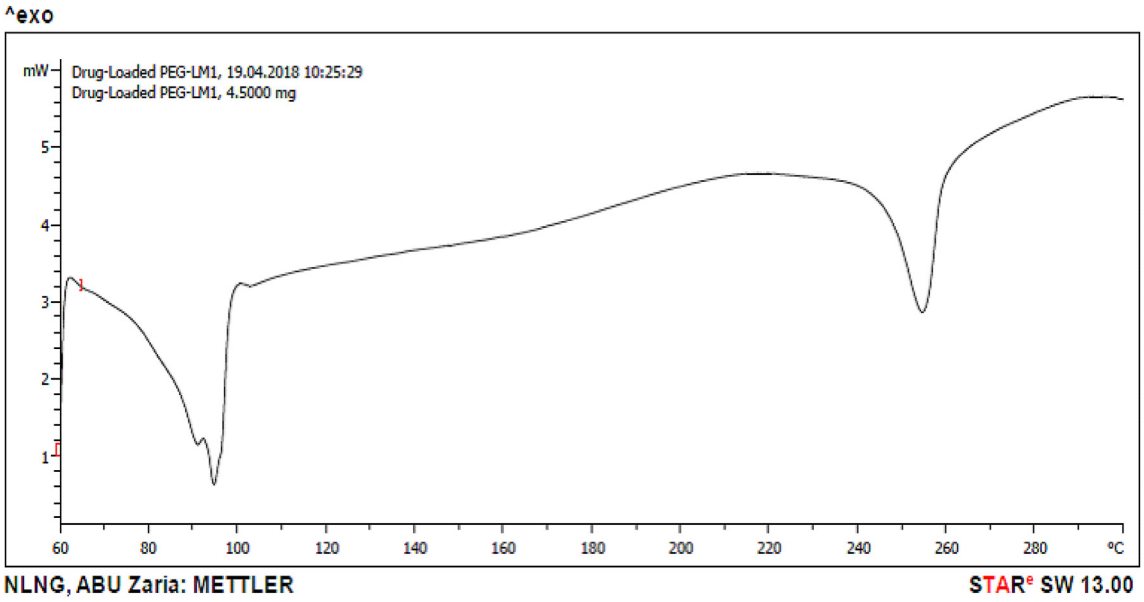

Figure 8. Differential scanning calorimetry (DSC) thermogram of metformin-loaded PEGylated lipid matrix (Drug-loaded PEG-LM_1).

the literature on the use of PEGylated solid lipid nanoparticles for oral delivery of metformin for enhanced treatment of diabetes mellitus. Nano-sized formulations offer tremendous benefits over conventional PEGylated systems. Therefore, the investigation of PEGylated lipid nanoparticles for enhanced metformin delivery to optimize the efficacy, intestinal absorption, bioavailability, biological half-life, and reduce drug dose, dosing frequency and drug adverse effects, informs the aim of this study. Thus, the objective of this study was to formulate, characterize and evaluate *in vitro and in vivo* pharmacodynamic properties of metformin–loaded beeswax based PEGylated solid lipid nanoparticles (PEG-SLN) for improved delivery of metformin hydrochloride.

2. Materials and methods

2.1. Materials

Metformin hydrochloride pure sample was obtained as a gift from May and Baker PLC (Ikeja, Lagos State, Nigeria). Phospholipon® 90H (P90H) (Phospholipid GmbH, Köln, Germany), sorbitol (Caesar & Loretz, Hilden, Germany), polyethylene glycol 4000 (PEG 4000) (Ph. Eur. Carl Roth GmbH + Co. KG Karlsruhe, Germany), beeswax (Carl Roth, Karlsruhe, Germany), Polysorbate 80 (Tween® 80) (Acros Organics, Geel, Belgium), Alloxan (Merck KGaA, Darmstadt, Germany), Glucophage® (Merck), distilled water (Lion water, University of Nigeria, Nsukka, Nigeria) and other solvents and reagents were used as procured from their manufacturers without further purification. Adult albino Wistar rats of both sexes were procured from the Faculty of Veterinary Medicine, University of Nigeria, Nsukka.

2.2. Methods

2.2.1. Preparation of non-PEGylated and PEGylated lipid matrices

The base lipid matrices were prepared by fusion method [43] using beeswax (BW) and Phospholipon® 90H (P90H) followed by PEGylation. The lipids were used at 7:3 ratio (i.e., 21.0 g of beeswax and 9.0 g of Phospholipon® 90H (P90H). Briefly, 21.0 g of beeswax and 9.0 g of P90H were weighed using an electronic balance (Mettler H8, Switzerland), poured into a crucible and melted together at 70 °C on a

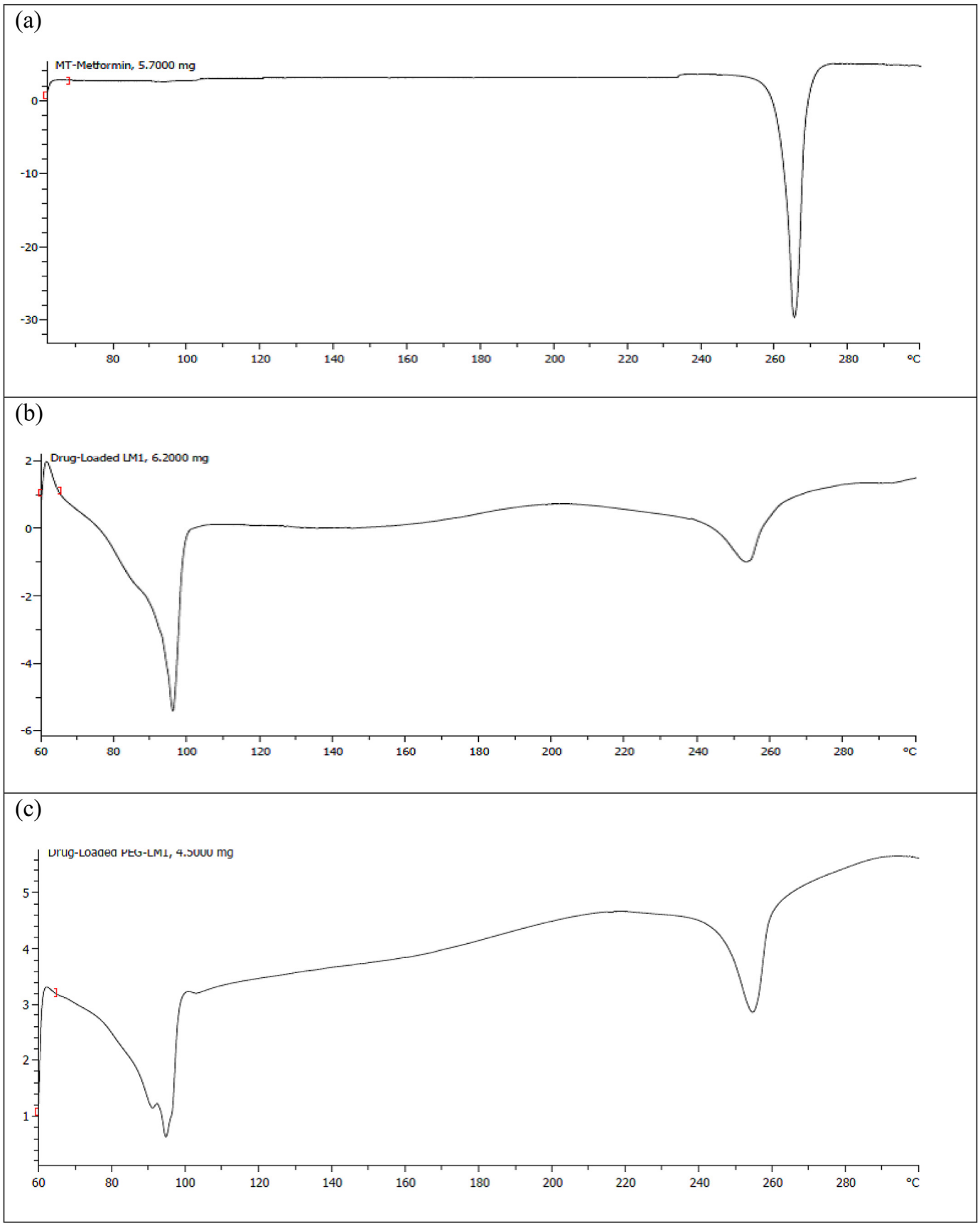

Figure 9. DSC thermographs of MT (a) and MT-loaded non-PEGylated and PEGylated lipid matrices (Drug-loaded LM_1) and (Drug-loaded PEG-LM_1) (b and c) in superposition.

Table 3. Thermal properties (DSC profiles) of PEG-4000, drugs, plain and drug-loaded lipid matrices.

Sample	Melting peak (°C)	Enthalpy (mW/mg)	Type of peak
Beeswax	73	-55.3	Endothermic
Phospholipon® 90H (P90H)	122.1	-38.9	Endothermic
LM_1	88.6	-32.5	Endothermic
PEG-4000	74.5	-3.8	Endothermic
PEG-LM_1	94.3	-14.2	Endothermic
Metformin	265.5	-28.4	Endothermic
LM_1+Drug	97.4	-5.4	Endothermic
	252.3	-0.8	Endothermic
PEG-LM_1+Drug	95.4	-0.4	Endothermic
	254.5	3.4	Exothermic

thermo-regulated oil bath (liquid paraffin) and stirred thoroughly to obtain an adequate mixing until a homogenous, transparent white mixture was obtained. The homogenous mixture of the lipid matrix was stirred further at room temperature and then allowed to cool and solidify. After 24 h, various quantities (90, 80 and 60% w/w) of the prepared lipid matrix were melted in the thermo-regulated bath at a temperature of 80 °C, together with corresponding amounts of polyethylene glycol (PEG 4000) (10, 20 and 40% w/w) incorporated at 80 °C over the oil bath to give PEGylated lipid matrices containing 1:9, 2:8, 4:6 ratios of PEG: lipid matrix, respectively, which were stirred properly and allowed to solidify. The non-PEGylated and PEGylated lipid matrices were thereafter stored in airtight and moisture resistant glass bottles away from light.

2.2.2. Preparation of drug-loaded non-PEGylated and PEGylated lipid matrices

Representative drug-loaded non-PEGylated and PEGylated lipid matrices were prepared by fusion using the non-PEGylated and PEGylated lipid matrices and metformin. With target non-PEGylated and PEGylated lipid concentration of 5.0% w/w and target drug concentrations of 1.0% w/w of metformin in the non-PEGylated and PEGylated solid lipid nanoparticle to be developed, 2.5 g of each of the lipid matrices was melted in the thermo-regulated oil bath at a temperature of 80 °C followed by addition of 0.5 g of metformin. Each of the mixture was stirred continuously until a homogenous, transparent white melt was gotten. The homogenous mixtures of the drug-loaded lipid matrices (MT-loaded LM_1 and MT-loaded PEG-LM_1) were stirred further at room temperature and allowed to solidify after which they were stored in airtight and moisture resistant glass bottle in the refrigerator.

2.2.3. Differential scanning calorimetry (DSC) analysis of plain and drug-loaded non-PEGylated and PEGylated lipid matrices

Thermal properties of beeswax, Phospholipon® 90H (P90H), beeswax-based P90H-modified lipid matrix (LM_1), PEG 4000, PEGylated beeswax-based P90H-modified lipid matrix (PEG-LM_1), metformin and metformin-loaded non-PEGylated and PEGylated beeswax-based P90H-modified lipid matrices (MT-loaded LM_1 and MT-loaded PEG-LM_1) were determined using a differential scanning calorimeter (DSC Q100 TA Instrument, Germany). Approximately 5 mg of each sample was weighed into an aluminum pan, hermetically sealed and the thermal behavior determined in the range of 20–350 °C at a heating rate of 5 °C/min. The temperature was maintained at 80 °C for 10 min and thereafter, cooled at the rate of 5–10 °C/min. Before the determinations, baselines were determined using an empty pan, and all the thermograms were baseline-corrected.

2.2.4. Fourier transform infra-red (FT-IR) spectroscopic analysis of drug-loaded non-PEGylated and PEGylated lipid matrices

The spectroscopic analysis was conducted on metformin and representative metformin-loaded non-PEGylated and PEGylated beeswax-based P90H-modified lipid matrices (MT-loaded LM_1 and MT-loaded PEG-LM_1) using a Shimadzu FT-IR 8300 Spectrophotometer (Shimadzu, Tokyo, Japan) adopting a wavelength in the region of 4000 to 400 cm^{-1} with threshold of 1.303, sensitivity of 50 and resolution of 2 cm^{-1} range. Data collection was performed using a smart attenuated total reflection (SATR) accessory. For baseline scanning, potassium bromate (KBr) plate was employed after thorough cleaning with a tri-solvent (acetone–toluene–methanol at 3:1:1 ratio) mixture. Approximately 0.1 g of each sample was mixed with 0.1 ml nujul diluent, introduced into the KBr plate and compressed into discs by applying a pressure of 5 tons for 5 min in a hydraulic press. The pellets were placed in the light path and the spectra collected in 60 s using Gram A1 spectroscopy software, and the chemometrics were performed using TQ Analyzer 1.

2.2.5. Preparation of non-PEGylated and PEGylated solid lipid nanoparticles

Non-PEGylated and PEGylated solid lipid nanoparticles encapsulating metformin (J_0, J_{10}, J_{20}, J_{40}) were prepared using the drug, non-PEGylated and PEGylated lipid matrices, Polysorbate® 80 (Tween® 80) (mobile surfactant), sorbitol (cryoprotectant) and distilled water (vehicle) by the high shear hot homogenization method [26,44]. Briefly, specified quantity of each of the lipid matrix (5% w/w of the PEG-SLN formulations) was placed in glass beaker and melted at 80 °C in the temperature-regulated heater (IKA instrument) and the drug (1.0% w/w of metformin) was added to the melted lipid matrix. At the same time, an aqueous surfactant solution consisting of sorbitol (4% w/w) and polysorbate® 80 (2% w/w) were prepared in a separate beaker and heated at the same temperature. The hot aqueous surfactant phase was then dispersed in the hot lipid phase (oily phase) using an Ultra-Turrax T25 (IKA-Werke, Staufen, Germany) homogenizer at 1000 rpm for 5 min. The obtained pre-emulsions were homogenized at 15,000 rpm for 30 min, and allowed to cool or re-crystallize at room temperature. The formulation compositions of the non-PEGylated and PEGylated lipid matrices as well as the formulation compositions of the non-PEGylated and PEGylated SLNs are shown in Table 1 and Table 2, respectively.

2.2.6. Characterization of the non-PEGylated and PEGylated SLNs

2.2.6.1. Particle size and polydispersity indices. The particle properties [average particle diameter, Z. Ave (nm) and polydispersity indices (PDI)] of the formulations were measured using a zeta sizer nano-ZS (Malvern Instrument, Worceshtire, UK) equipped with a 10 mw He-NE laser employing the wavelength of 633 nm and a backscattering angle of 173° at 25 °C. Before the photon correlation spectroscopic (PCS) analysis, each sample was diluted with double-distilled water to obtain a suitable scattering intensity.

2.2.6.2. Scanning electron microscopy (SEM). The morphological characteristics of the formulations (representative batch) were determined by a scanning electron microscope (JEOL-JSM-6 360, Japan) at different magnifications. One drop of sample was placed on a slide and excess water was left to dry at room temperature. The slide was attached to the specimen holder using double coated adhesive tape and gold coating under vacuum using a sputter coater (Model JFC-1100, JEOL, Japan) for 10 min, and then investigated at 20 kV.

2.2.6.3. Compatibility study by fourier transform infra-red (FT-IR) spectroscopy. The procedure for the FT-IR analysis of the non-PEGylated and PEGylated SLNs is same as stated in section 2.2.4 except that a 0.1 ml volume of each of the formulation was mixed with 0.1 ml nujul diluent and introduced into the KBr plate and compressed into discs by applying a pressure of 5 tons for 5 min in a hydraulic press.

2.2.6.4. Encapsulation efficiency determination. The encapsulation efficiency of each formulation was determined. A 5 ml volume of each solid lipid nanoparticles dispersion was placed in a centrifuge tube and was centrifuged for 30 min at an optimized speed of 4000 rpm in order to obtain two phases (the aqueous phase and lipid phase). A 1 ml volume of

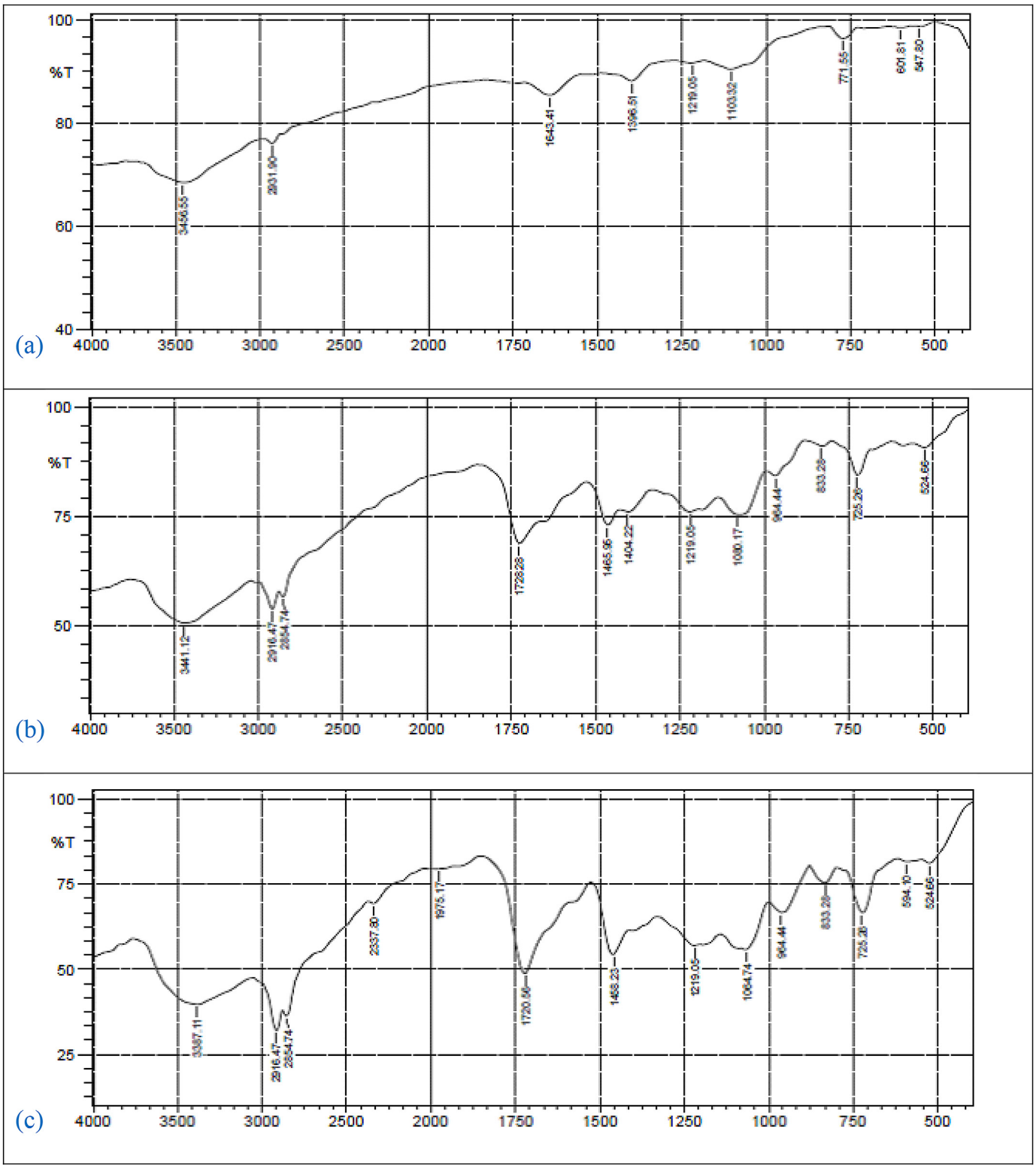

Figure 10. FT-IR spectra of MT (a) and MT-loaded beeswax-based non-PEGylated and PEGylated lipid matrices (Drug-loaded LM_1) and (Drug-loaded PEG-LM_1) (b and c) in superposition.

the aqueous phase was measured with the aid of a syringe and then diluted 10,000-fold using distilled water. The absorbance of the dilutions was taken using a UV spectrophotometer (JENWAY 6405, UK) at a wavelength of 231.5 nm and the amount of drug encapsulated in the PEG-SLNs was calculated with reference to standard Beer-Lambert's plot for metformin to obtain the EE % using Eq. (1) [45].

$$EE\% = \frac{Actual\ drug\ content}{Theoritical\ drug\ content} \times 100\% \quad (1)$$

2.2.6.5. Loading capacity. Loading capacity of drug in lipid carriers depends on the type of lipid matrix, solution of drug in melted lipid, miscibility of drug melt and lipid melt, chemical and physical structure of

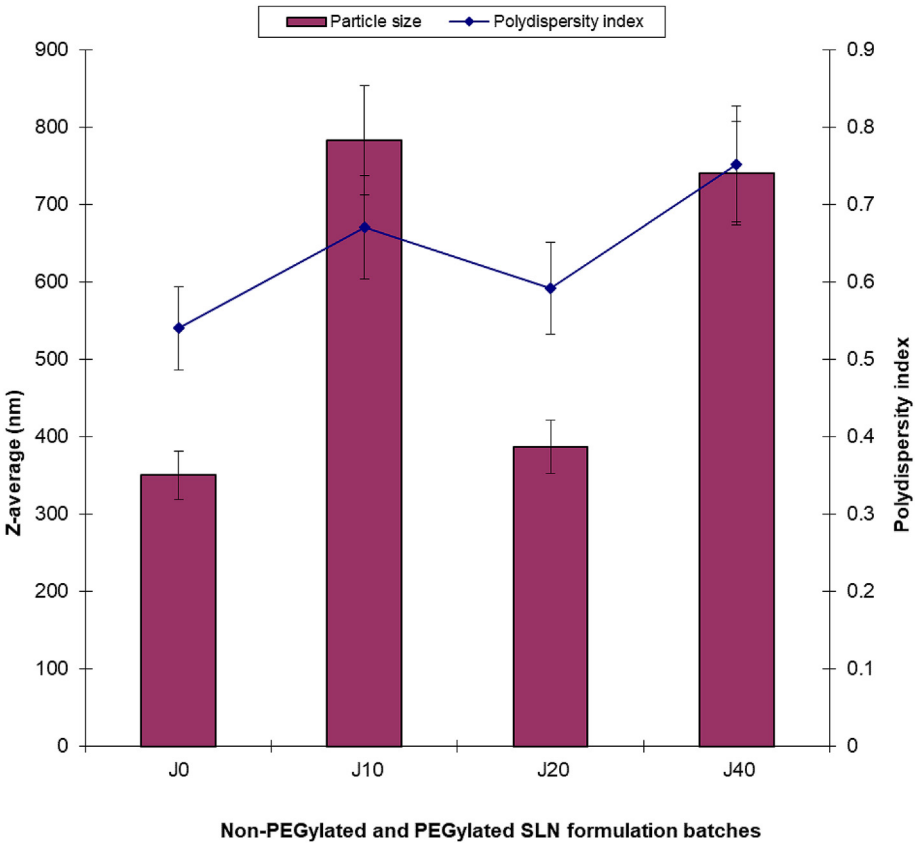

Figure 11. Combined particle size analysis result of the metformin-loaded beeswax-based non-PEGylated and PEGylated solid lipid nanoparticles.

solid lipid matrix and the polymorphic state of the lipid material [43]. Loading capacity (LC) is expressed as the ratio between the entrapped drug by the lipid and the total quantity of the lipids used in the formulation [5]. It was calculated using Eq. (2).

$$Loading\ capacity = \frac{Total\ quantity\ of\ drug\ entrapped\ by\ the\ lipid}{Total\ quantity\ of\ lipid\ in\ the\ formulation} \times 100\% \quad (2)$$

2.2.6.6. In vitro drug release study. The USP XXII rotating paddle apparatus (Erweka, GmbH Germany) was employed for this release study. The dissolution medium consisted of 500 mL of freshly prepared phosphate buffer maintained at 37±1 °C by means of a thermo-regulated water bath. The polycarbonate dialysis membrane used as a release barrier was pre-treated by soaking it in the dissolution medium for 24 h prior to the commencement of each release experiment. In each case, 2 ml of the drug loaded PEGylated NLC was placed in the dialysis membrane, securely tied with a thermo-resistant thread and then immersed in the dissolution medium under agitation provided by the paddle at 200 rpm. At predetermined time intervals (0.5, 1, 2, 3, 4, 5, 6, 7 and 8 h), 5mL portions of the dissolution medium were withdrawn and replaced with equal volume of the medium to maintain a sink condition, filtered with a pore size of 0.22 mm (Millipore filter, Delhi, India) and analysed using a spectrophotometer (Jenway, UK) at 231.5 nm.

2.2.6.7. In vivo antidiabetic study

2.2.6.7.1. Ethical approval and experimental animals. All applicable international, national and/or institutional guidelines for the care and use of animals were followed. All experimental protocols were conducted with strict adherence to the guidelines of the Faculty of Pharmaceutical Sciences Animal Care and Use Committee of the University of Nigeria, Nsukka. in line with the International Code of Practice for the care and use of animals for scientific purposes. Ethical clearance approval for *in vivo* antidiabetic studies was sought and obtained from the Faculty of Pharmaceutical Sciences Research Ethics Committee (UNN/FPS/2019–2020_016X) before the commencement of the *in vivo* animal studies.

Wistar albino rats of both sexes weighing between 150 to 200 g were bred in the Faculty of Veterinary medicine, University of Nigeria, Nsukka. The animals were housed in standard environmental conditions, kept at body temperature of 37 ± 1 °C using warming lamps and left for one week to acclimatize with the new laboratory environment while

Figure 12. Representative of the morphology scanning electron micrograph, (SEM) of metformin-loaded PEGylated solid lipid nanoparticles (batch J_{20}).

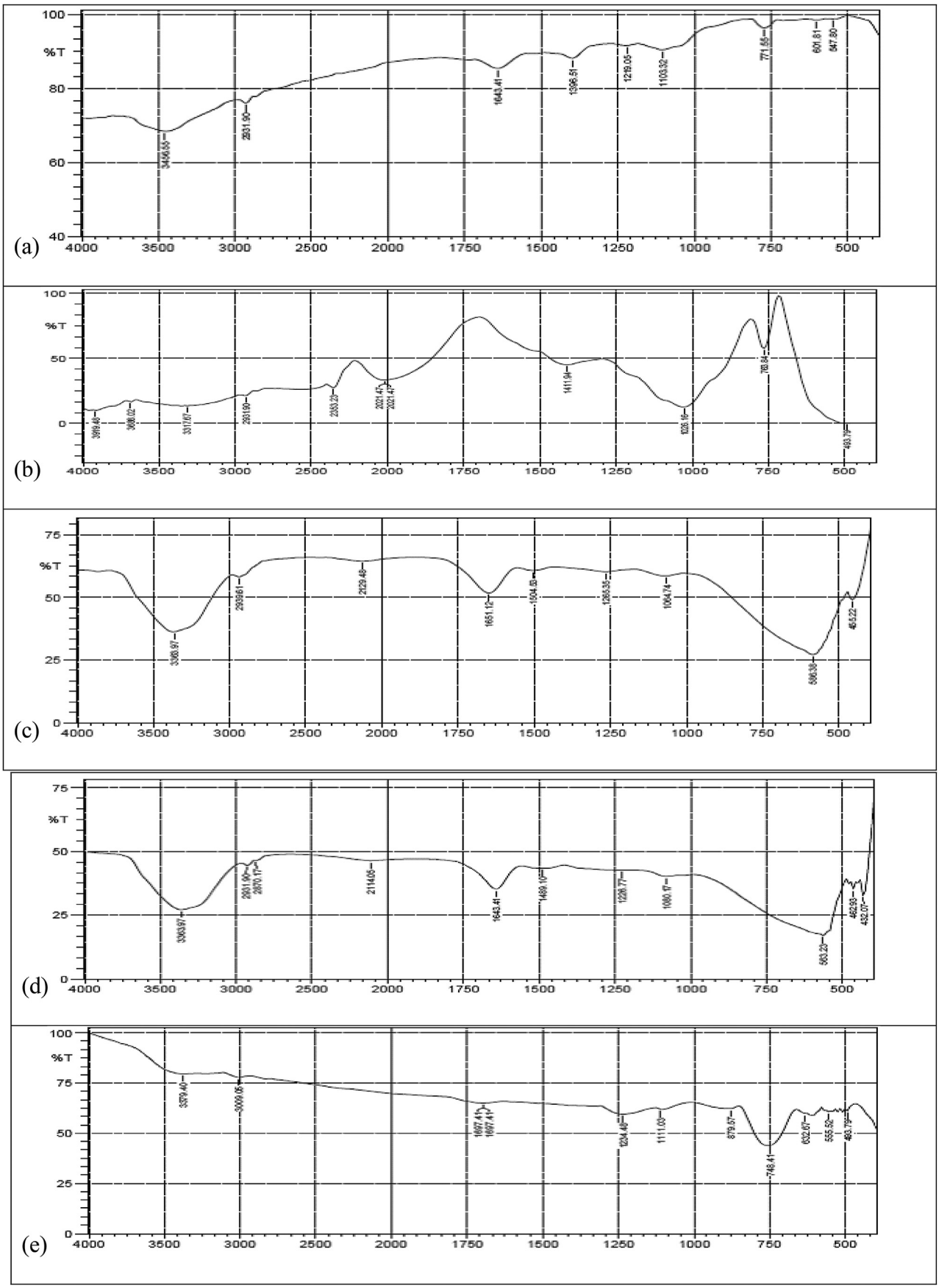

Figure 13. FT-IR spectra of MT (a) and MT-loaded beeswax-based non-PEGylated and PEGylated solid lipid nanoparticles (J_0, J_{10}, J_{20} and J_{40}) (b–e) in superposition.

Table 4. Encapsulation efficiency and loading capacity of PEGylated and non-PEGylated SLNs.

Formulation	Encapsulation Efficiency (%)	Loading capacity
J_0	97.71 ± 3.58	16.35 ± 1.87
J_{10}	97.51 ± 2.49	16.32 ± 3.63
J_{20}	99.28 ± 4.01	16.57 ± 2.54
J_{40}	97.55 ± 2.96	16.33 ± 0.98

being fed with standard laboratory diet. All the animals were fasted for 12 h, but were allowed free access to water, before commencement of the experiments.

2.2.6.7.2. Induction of experimental diabetes. Adult Wistar rats (either sex) were used for the evaluation of the anti-diabetic effects of the formulations. The rats were divided into groups of six animals each and each group of animals was housed in a separate cage. Diabetes was induced by single intraperitoneal injection of a freshly prepared solution of alloxan (150 mg/kg) in normal saline for all the groups. After 1 h of alloxan administration, the animals were fed freely and 5% dextrose solution was also given orally in a feeding bottle for a day to overcome the early hypoglycaemic phase. The animals were kept under observation, and after 48 h, blood was withdrawn from the tail vein of the animals and the blood glucose level measured with a glucometer (Accu-check, Roche, USA). The diabetic rats (glucose level above 200 mg/dl) were separated and divided into ten different groups (n = 6).

2.2.6.7.3. Evaluation of anti-diabetic activity. Sixty diabetic Wistar rats (either sex) were used for the evaluation of the anti-diabetic effects of the formulations. The sample batches of the different formulations of the metformin-loaded non-PEGylated and PEGylated SLN were administered orally to the animals according to their weight as follows:

- Group A: received the test formulation (batch J_0) equivalent to 100 mg/kg dose of metformin hydrochloride.
- Group B: received the test formulation (batch J_{10}) equivalent to 100 mg/kg dose of metformin hydrochloride.
- Group C: received the test formulation (batch J_{20}) equivalent to 100 mg/kg dose of metformin hydrochloride.
- Group D: received the test formulation (batch J_{40}) equivalent to 100 mg/kg dose of metformin hydrochloride.
- Group E: received the test formulation (batch J_{10}) equivalent to 50 mg/kg dose of metformin hydrochloride.
- Group F: received the test formulation (batch J_{20}) equivalent to 50 mg/kg dose of metformin hydrochloride.
- Group G: received the test formulation (batch J_{40}) equivalent to 50 mg/kg dose of metformin hydrochloride.
- Group H: received Glucophage® equivalent to 100 mg/kg dose of metformin hydrochloride (first positive control).
- Group I: received pure metformin equivalent to 100 mg/kg dose of metformin hydrochloride (second positive control).
- Group J: received normal saline per orally (negative control).

Blood samples of the animals were collected from the tail vein afterwards at time intervals of 0, 1, 3, 6, 12, and 24 h and tested for blood glucose level using the glucometer. The post-dose levels of the blood glucose were expressed as a percentage of the pre-dose level using Eq. (3).

Table 5. *In vitro* kinetics of release of metformin from PEG-SLN in phosphate buffer.

Batch Code	Zero order (r^2)	First order (r^2)	Higuchi square root (r^2)	Korsmeyer–Peppas	
				(r^2)	n
Glucophage	1.0000	0.8820	0.9827	0.9954	0.76
J_0	1.0000	0.8669	0.9768	0.9938	0.83
J_{10}	1.0000	0.8681	0.9778	0.9939	0.82
J_{20}	0.9999	0.8829	0.9819	0.9954	0.76
J_{40}	1.0000	0.8843	0.9824	0.9956	0.76

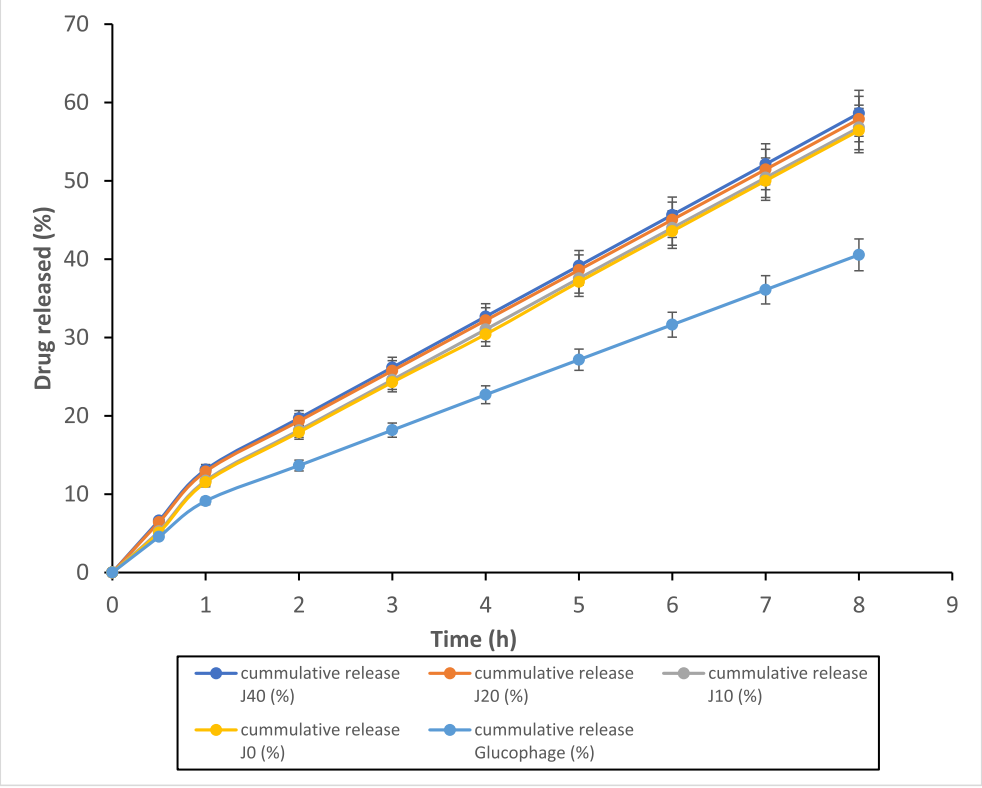

Figure 14. *In vitro* drug dissolution profile of metformin, metformin-loaded non-PEGylated and PEGylated beeswax-based SLNs.

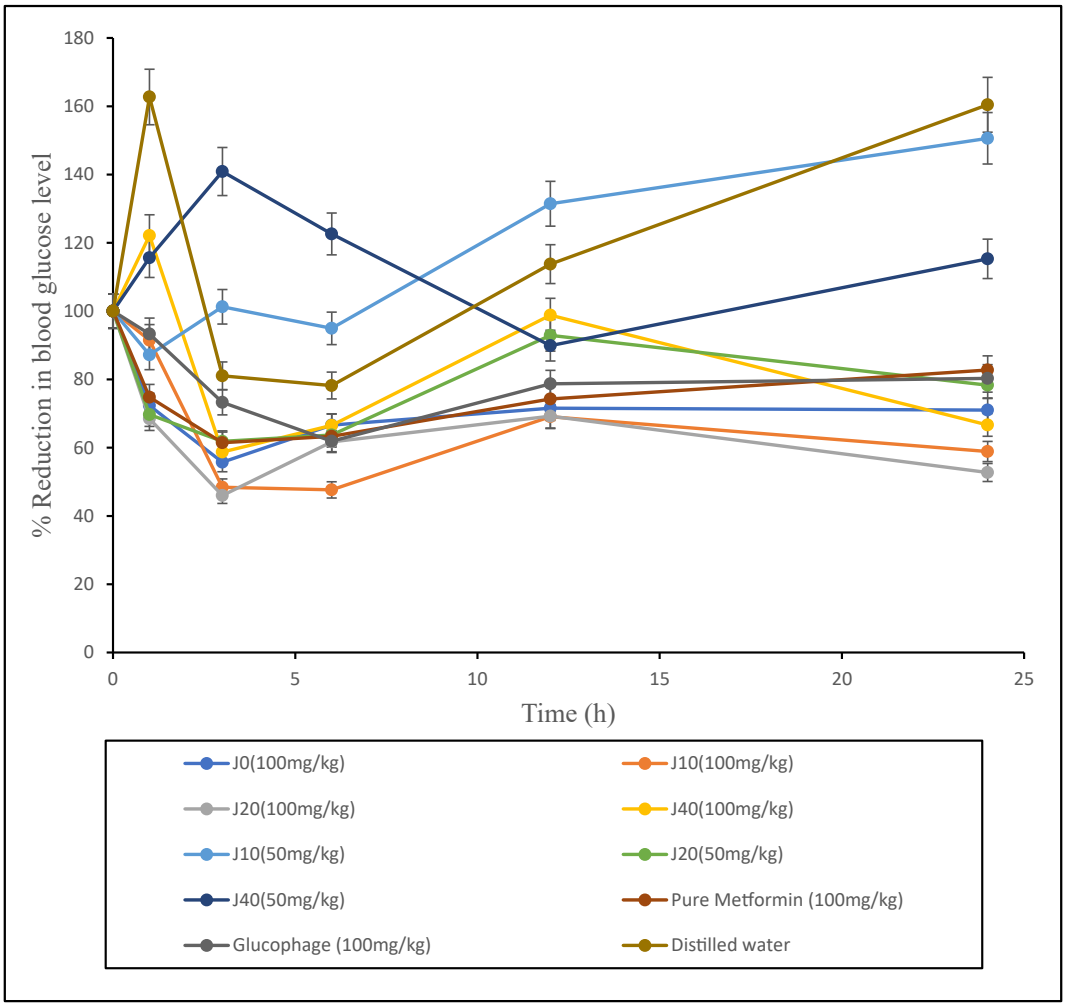

Figure 15. Graphical representation of the *in vivo* antidiabetic effect (blood glucose lowering effect) of the non-PEGylated and PEGylated beeswax-based formulations.

$$\%glycemic\ change = \frac{Initial\ conc\ - Final\ conc}{Initial\ conc} \times 100\% \quad (3)$$

2.2.7. Statistical analysis

All experiments were performed in replicates for validity of statistical analysis. Results were expressed as mean ± SEM. Analysis of variance (ANOVA) was performed on the data sets generated using Statistical Package for Social Sciences (SPSS) software 16.0. Differences were considered significant for p-values < 0.05.

3. Results and discussion

3.1. Thermal properties of plain and drug-loaded lipid matrices

Figures 1, 2, 3, 4, 5, 6, 7, 8, 9 shows the DSC thermogram of beeswax, Phospholipon® 90H, structured lipid matrix (LM_1), PEG 4000, PEGylated lipid matrix, metformin, metformin-loaded lipid matrix (Drug-loaded PEG-LM_1) and metformin-loaded PEGylated lipid matrix (Drug-loaded LM_2) while Table 3 shows the thermal properties of the drug, lipids, PEG 4000 and all the matrices. Polymorphic transition and crystallization temperature of lipids used in the formulation of SLNs are important parameters. For amorphous substances or crystals that are less ordered, lesser energy is required to melt the substance than in a substance with perfect crystalline structure in which higher energy is required to overcome lattice forces. Therefore, higher melting enthalpy values would suggest a higher ordered lattice arrangement [46]. The slight presence or total absence of a melting peak in the DSC of a pharmaceutical formulation indicates that the drug is partly or completely amorphous/molecularly dispersed [47,48]. Metformin and Phospholipon® 90H thermograms showed a single sharp endothermic peak at 265.5 and 122.1 °C with enthalpy of -28.4 and -38.9 mW/mg, respectively, corresponding to their melting points, an indication of the highly crystalline nature of these materials. The DSC thermograms of beeswax and PEG 4000 showed melting peak at 73 and 74.5 °C with enthalpy of -55.3 and -3.8 mW/mg, respectively, indicating their crystalline nature. However, the thermograms of LM_1 and PEG-LM_1 showed melting peaks at 88.6 and 94.3 °C with enthalpies at -32.5 and -14.2 mW/mg respectively, this indicates that lipid matrices are less crystalline than the individual components used in the formulation due to their lower enthalpy values. This means that there is a distortion of the crystal arrangement of the lipids after melting and solidification thus generating an imperfect matrix leaving spaces for drug encapsulation. The DSC thermogram of the drug-loaded lipid matrix (LM_1+Drug) and metformin-loaded PEGylated lipid matrix (drug loaded PEG-LM_2) showed two melting peaks each. The drug-loaded lipid matrix (LM_1+Drug) showed endothermic peak at 97.4 and 252.3 °C, the second peak at 252.3 °C was a weak peak showing that metformin is either partly amorphous or molecularly dispersed in the lipid matrix. The metformin-loaded PEGylated lipid matrix (drug loaded PEG-LM_1) also showed two peaks, one endothermic peak at 95.4 °C with enthalpy of -0.4 mW/mg and an exothermic peak at 254.5 °C with enthalpy of 34 mW/mg. The exothermic peak at 254.5 °C could be due to the molecules arranging themselves to a lower energy configuration or due to chemical cure.

Table 6. Blood glucose level of the treatment groups.

Group	Treatment	FBS pre induction (mg/dl)	0 h	1 h	3 h	6 h	12 h	24 h
1	J_0 (100 mg/kg)	102.25 ± 7.96	228.30 ± 46.73	170.70 ± 45.91 (27.66%)	130.30 ± 33.71 (44.27%)	160.00 ± 49.52 (33.39%)	166.00 ± 38.59 (28.44%)	**161.70 ± 35.59 (28.99%)
2	J_{10} (100 mg/kg)	83.25 ± 4.44	244.00 ± 42.72	252.30 ± 129.20 (8.53%)	131.00 ± 71.51 (51.57%)	127.00 ± 60.22 (52.35%)	176.70 ± 52.42 (30.95%)	**152.30 ± 64.86 (41.12%)
3	J_{20} (100 mg/kg)	74.50 ± 9.65	248.80 ± 19.09	169.00 ± 24.84 (31.52%)	117.80 ± 30.22 (54.02%)	159.50 ± 48.07 (38.32%)	169.50 ± 26.55 (30.77%)	**130.00 ± 21.83 (30.77%)
4	J_{40} (100 mg/kg)	87.75 ± 11.35	228.00 ± 21.07	268.00 ± 29.51 (-22.12%)	138.70 ± 48.63 (41.28%)	156.30 ± 45.31 (33.47%)	233.70 ± 74.14 (1.18%)	**154.70 ± 53.74 (33.34%)
5	J_{10} (50 mg/kg)	76.75 ± 5.31	268.00 ± 43.02	220.30 ± 11.05 (12.80%)	256.70 ± 10.17 (-1.27%)	241.00 ± 8.963 (5.05%)	331.00 ± 20.84 (-31.45%)	372.70 ± 81.28 (-50.62%)
6	J_{20} (50 mg/kg)	59.75 ± 2.95	290.30 ± 15.60	201.70 ± 7.80 (30.27%)	178.30 ± 10.48 (38.16%)	184.00 ± 15 (36.26%)	270.70 ± 24.92 (7.07%)	*229.30 ± 31.07 (21.68%)
7	J_{40} (50 mg/kg)	71.50 ± 3.66	374.00 ± 107.2	400.70 ± 56.88 (-15.64%)	483.30 ± 54.14 (-40.88%)	407.70 ± 32.42 (-22.62%)	273.30 ± 94.18 (10.10%)	363.30 ± 95.97 (-15.30%)
8	Glucophage (100 mg/kg)	76.50 ± 6.03	230.00 ± 12.66	221.70 ± 79.45 (6.71%)	175.70 ± 77.37 (26.73%)	148.00 ± 63.04 (38.10%)	184.70 ± 55.85 (21.30%)	**189.30 ± 59.40 (19.70%)
9	Pure metformin (100 mg/kg)	85.25 ± 14.61	313.00 ± 23.12	235.70 ± 28.35 (25.23%)	193.30 ± 20.25 (38.52%)	203.00 ± 46.87 (36.66%)	236.00 ± 46.18 (25.73%)	*260.00 ± 29.09 (17.25%)
10	Distilled water	67.00 ± 5.94	259.70 ± 15.17	411.30 ± 99.91 (-62.74%)	210.70 ± 34.45 (18.94%)	203.70 ± 29.54 (21.79%)	292.70 ± 22.15 (-13.75%)	408.00 ± 90.36 (-60.44%)

Values are expressed as mean ± SEM, n = 6, ** = p <0.05 (very significant) and * = p <0.05 (significant) vs. Negative control (Distilled water treated) group. Values in parenthesis denote percentage reduction of blood glucose.

3.2. Fourier transform infra-red spectroscopy of drug and drug-loaded lipid matrices

FT-IR spectroscopic analysis is usually carried out to evaluate any possible molecular interactions between the drug and the matrices in the solid state [49]. The infrared (IR) spectrum of any given compound is always unique and characteristic of that compound [31]. The FT-IR spectra of metformin, metformin-loaded lipid matrix (MT-loaded LM_1) and metformin-loaded PEGylated lipid matrix (MT-loaded PEG-LM_1) are presented in Figure 10. The FT-IR spectrum of pure metformin sample showed principal characteristic absorption bands at 3456.55 cm^{-1} (N–H stretching), 2931.90 cm^{-1} ($(CH_3)_2$–N absorption), 1643.41 cm^{-1} (N–H deformation), 1396.51 cm^{-1} (N–H deformation), 1219.05 cm^{-1} (C–O vibration), 1130.74 cm^{-1} (C–N stretching), 1103.32 cm^{-1} (C–N stretching), 771.56 cm^{-1} (N–H wagging), 601.81 cm^{-1} (C–H out of plane bending) and 547.8 cm^{-1} (C–N–C deformation). The FT-IR spectra of metformin-loaded lipid matrix (MT-loaded LM_1) showed principal characteristic absorption bands of metformin at 3441.12 cm^{-1} (N–H stretching), 2916.47 cm^{-1} ($(CH_3)_2$–N absorption), 2854.74 cm^{-1} ($(CH_3)_2$–N absorption), 1728.28 cm^{-1} (conjugated C=C bond vibration), 1465.95 cm^{-1} (symmetric N–H deformation), 1404.22 cm^{-1} (N–H deformation), 1219.05 cm^{-1} (C–O vibration), 1080.17 cm^{-1} (C–N stretching), 964.44 cm^{-1} (N–H out of plane bending), 833.28 cm^{-1} (NH_2 rocking), 725.26 cm^{-1} (C–H out of plane bending) and 524.66 cm^{-1} (C–N–C deformation). The FT-IR spectra of metformin-loaded PEGylated lipid matrix (MT-loaded PEG-LM_1) showed principal characteristic absorption bands of metformin at 3387.11 cm^{-1} (N–H stretching), 2916.47 cm^{-1} ($(CH_3)_2$–N absorption), 2854.74 cm^{-1} ($(CH_3)_2$–N absorption), 2337.80 cm^{-1} (-C=C- stretching), 1975.17 cm^{-1} (aromatic –C=O bond vibration), 1720.56 cm^{-1} (conjugated C=C bond vibration), 1458.23 cm^{-1} (N–H deformation), 1219.05 cm^{-1} (C–O vibration), 1064.74 cm^{-1} (C–N stretching), 964.44 cm^{-1} (N–H out of plane bending), 833.28 cm^{-1} (NH_2 rocking), 725.26 cm^{-1} (C–H out of plane bending), 594.10 cm^{-1} (C–N–C deformation) and 524.66 cm^{-1} (C–N–C deformation). The peak intensity of vibrations in the metformin-loaded lipid matrix and metformin-loaded PEGylated lipid matrix may be reduced due to the presence of hydrogen bonding [50]. All the characteristic peaks of metformin were present, although some had slightly reduced intensity, signifying that there was no significant chemical interaction between the drug-lipid or drug-polymer [51]. The presence of other peaks in the FT-IR spectra of metformin-loaded lipid matrices indicates the presence of the polymer (PEG 4000) and the lipids (beeswax and Phospholipon® 90H).

3.3. Mean particle size and polydispersity indices of the SLNs formulations

The combined particle size analysis and polydispersity index of the formulations is shown in Figure 11. The solid lipid nanoparticles size was found to be minimum (350.00 nm) for J_0 and maximum (783.10 nm) for the J_{10} batch. The PDI value of batch J_0 and J_{40} was found to be 0.54 and 0.752 showing the minimum and maximum PDI in the formulation respectively. The particle size distribution was normal and this was confirmed by the polydispersity index. These results showed a unimodal size distribution of the different particle sizes, indicating that the formulations are stable [5]. Polydisperse systems have greater tendency to aggregation than monodisperse system thus J_0 is the most stable formulation.

3.4. Scanning electron microscopy (SEM) of drug-loaded non-PEGylated and PEGylated solid lipid nanoparticles

Figure 12 shows the image obtained for J_{20} (representative formulation) by SEM. The image showed that the particles were segregated, uniform in size and spherical/semi-spherical in shape which is the typical morphological aspects of nanoparticles.

3.5. Fourier transform infra-red spectroscopy of drug-loaded SLNs formulations

The FT-IR spectra of metformin, metformin-loaded beeswax-based non-PEGylated and PEGylated solid lipid nanoparticles (J_0, J_{10}, J_{20} and J_{40}) (b-e) in superposition are presented in Figure 13. The FT-IR spectrum of pure metformin sample showed principal characteristic absorption bands of metformin described previously. The FT-IR spectra of metformin-loaded non-PEGylated SLN (J_0) showed principal characteristic absorption bands of metformin at 3371.68 cm^{-1} (N–H stretching), 2060.04 cm^{-1} (carboxylic acid C=O vibration), 1643.41 cm^{-1}, 1550.82 cm^{-1}, 1411.94 cm^{-1} (N–H deformation), 1280.78 cm^{-1} (C–O vibration), 1072.46 cm^{-1} (C–N stretching), and 563.23 cm^{-1} (C–N–C deformation). The FT-IR spectra of metformin-loaded PEGylated SLN (J_{10}, J_{20}, J_{40}) showed principal characteristic absorption bands of metformin and is summarized as follows:

J_{10}: 3363.97 cm^{-1} (N–H stretching), 2939.61 cm^{-1} ($(CH_3)_2$–N absorption), 2129.48 cm^{-1} (Carboxylic acid C=O vibration), 1651.12 cm^{-1} (N–H deformation), 1504.53 cm^{-1} (N–H deformation), 1265.35 cm^{-1} (C–O vibration), 1064.74 cm^{-1} (C–N stretching) and 586.38 cm^{-1} (C–N–C deformation). J_{20}: 3363.97 cm^{-1} (N–H stretching), 2931.90 cm^{-1}, 2870.17 cm^{-1} ($(CH_3)_2$–N absorption), 2114.05 cm^{-1} (Carboxylic acid C=O vibration), 1643.41 cm^{-1} (N–H deformation), 1489.10 cm^{-1} (symmetric N–H deformation), 1226.77 cm^{-1} (C–O vibration), 1080.17 cm^{-1} (C–N stretching) and 563.23 cm^{-1} (C–N–C deformation). J_{40}: 3379.40 cm^{-1} (N–H stretching), 3009.05 cm^{-1} ($(CH_3)_2$–N absorption), 1697.41 cm^{-1} (N–H deformation), 1234.48 cm^{-1} (C–O vibration), 1111.03 cm^{-1} (C–N stretching), 879.57 cm^{-1} (NH_2 rocking), 748.41 cm^{-1} (N–H wagging), 632.67 cm^{-1} (C–H out of plane bending) and 586.38 cm^{-1} (C–N–C deformation). Overall FT-IR results suggested the presence of no incompatibility between metformin and the excipients used in the formulation.

3.6. Encapsulation efficiency and loading capacity of PEGylated and non-PEGylated SLNs

The results of the encapsulation efficiency (EE%) and loading capacity (LC) of the SLNs are shown in Table 4. The encapsulation efficiencies were in the range of 97.51–99.28% for SLNs, with the formulation J_{20} showing the highest EE% while J_{10} had the least. However, all batches of the SLNs had good EE% (97.51–99.28%). The loading capacity of all the batches of SLNs showed similar pattern. The loading capacity (LC) of the SLN batches was in the range of 16.32–16.57 g of metformin per 100 g of lipid. The SLN batch J_{20} had the highest loading capacity while J_{10} had the least.

The drug loading efficiency could be affected by the drug's molecular weight, volumetric size of the carrier, chemical interactions between the drug and the carrier, solubility of the drug in the carrier and miscibility in the lipid matrix, and the lipid phase polymorphic state [17,20,52]. Increasing the crystalline order in the lipid matrices has a great impact on the drug loading capacity, since an increase in order reduces the ability to incorporate different molecules [20]. Thus, in order to decrease the degree of lipid phase crystallinity and to increase loading capacity, Phospholipon 90H (P90H), an amphiphilic phospholipid was incorporated into the lipid matrix. Metformin has a high tendency to escape from lipid matrix due to its high solubility in water [53] and may result in lower drug loading. PEG-lipids, when added in high concentration may induce formation of mixed micelles which may increase drug encapsulation efficiency [31]. This may account for the high encapsulation efficiency of the SLNs. Previous studies have shown a reverse relationship between particle size and loading parameters (loading efficiency and entrapment efficiency). Formulations with lower particle sizes had higher encapsulation efficiency and drug loading capacity, this is consistent with previous reports.

3.7. In vitro drug release from the metformin-loaded PEGylated and non-PEGylated SLNs

Figure 14 shows the release profiles of metformin from all the batches of PEG-SLN formulation in phosphate buffered solution (PBS, pH 7.4). The *in vitro* release profiles of metformin in PBS indicate significant release of metformin from all batches of the formulation. The different batches of the formulations showed high release rate in the trend $J_{40} > J_{20} > J_{10} > J_0$>Glucophage®. The release rate of the drug was higher in the formulations than the release in Glucophage®. Metformin was released in a controlled manner over time. Similar drug release pattern has been reported earlier [12]. This is expected as solid lipid nanoparticles slow down the mobility of drug out of the particles [54]. A study by Xu *et. al* also showed an initial rapid release of metformin from SLNs and chitosan modified SLN, which was predicted to be due to adsorption of metformin on the surface of the nanoparticles [55]. Also, as the concentration PEG 4000 polymer used in the formulation increased the rate of drug release increased. Thus, PEGylation enhanced the dissolution and release rate of the drug from the formulations.

In order to identify a particular release mechanism, experimental data of statistical significance were compared to a solution of the theoretical model [56]. Four different mathematical models were used to describe the kinetics of metformin release from the PEG-SLNs formulations. The most appropriate model of drug release was selected based on the goodness-of-fit test. The results showed that all the prepared formulations follow zero-order kinetics as shown in Table 5. The equation is of this model for batch J_{40} (representative sample) is

$$y = 6.4972x + 0.1697;\ r = 1.0000$$

Although the formulations showed good fit into zero order, Korsmeyer–Peppas, Higuchi and First order with good correlation coefficient ($r^2 \geq 0.8669$). Thus, the formulations predominantly followed the diffusion mechanism of drug release. While zero-order rate describes the systems where the drug release rate is independent of its concentration, first-order describes drug release from systems where the release rate is concentration-dependent. Higuchi kinetics describes drug release from systems where the drug is dispersed in an insoluble matrix as a square root of a time-dependent process based on Fickian diffusion [57]. Korsmeyer–Peppas model also known as power law describes drug release from a polymeric system. The n value obtained from Korsmeyer-Peppas plot is important since it is related to the mechanism of drug release (i.e., Fickian diffusion or non-Fickian diffusion). The values of n for all batches of the formulations were >0.5 and <1, which indicates the non-Fickian diffusion transport [58–60].

3.8. In vivo antidiabetic activity

The results of the anti-diabetic studies of the different nanoformulations administered orally to alloxan-induced diabetic rats, in comparison with the pure drug and commercially available product are shown in Figure 15 and Table 6. Figure 15 shows a chart representation of the percentage reduction in blood glucose whereas Table 6 shows the time course profile of blood glucose response in the rats. The antidiabetic activity of the nanoformulations were assessed by measuring the percentage reduction blood glucose concentration of the nano formulations (J_0, J_{10}, J_{20} and J_{40}), pure drug and commercially available product *in vivo*. The groups treated with 100 mg/kg of the J_0, J_{10}, J_{20} and J_{40} formulations showed higher and more sustained reduction in glucose level than those treated with the pure drug, which is an indication of improved performance produced by the nanoformulations, as shown in Figure 15. In animal groups treated with 100 mg/kg of these nanoformulations, the blood glucose reduction effectively commenced within an hour of oral administration; this may be attributed to high release rate of metformin adsorbed onto the surface of the lipid

nanoparticles: burst effect. The maximum blood glucose reduction (T_{max}) was achieved in 3 h in batch J_0, J_{20} and J_{40} and 6 h in batch J_{10} after which blood glucose level rose slightly. The percentage reduction in blood glucose level produced by the nanoformulations (J_{20}, J_{10}, J_0 and J_{40}) at these times reduced from 100% to 54.02, 52.35, 44.27 and 41.28%, respectively. Studies have shown that lipids and lipid-based excipients can influence oral absorption, bioavailability and disposition of drugs. This influence could be by altering the composition and character of the intestinal milieu, recruiting intestinal lymphatic drug transport, and interaction with enterocyte-based transport processes or other physiological effects, such as retarded gastric emptying [61]. Generally, the nanoformulations dosed at 100 mg/kg in comparison with pure metformin and the commercial sample, maintained the blood glucose level of the rats within the normoglycemic level for 24 h. This is consistent with similar study where metformin hydrochloride-loaded lipid vesicle showed significant reduction in blood glucose in alloxan-induced diabetic rats in a sustained pattern when compared with pure metformin hydrochloride [62].

4. Conclusion

The use of metformin for treatment of diabetes mellitus is limited by low bioavailability, short biological half-life, requirement for multiple daily doses, coupled with patient's requirement of life-long treatment and repeated administrations of doses thus reduced patient compliance. This study evaluates the potential of metformin–loaded beeswax based PEGylated solid lipid nanoparticles (PEG-SLN) for enhanced metformin delivery to treat diabetes mellitus. Metformin–loaded beeswax based PEGylated solid lipid nanoparticles (PEG-SLN) were successfully prepared by high shear hot homogenization method using structured lipids (beeswax and Phospholipon® 90H) and PEG 4000 and evaluated for improved treatment of diabetes mellitus. Solid-state characterization performed on the lipid matrices used in preparing the formulations confirmed the suitability of the lipid matrices and their compatibility with metformin. The present study suggests that PEGylated solid lipid nanoparticles are suitable carriers for oral delivery of metformin and other hydrophilic drugs. Hence by the application of these nanoformulations, bioavailability and duration of metformin can be increased for efficient treatment of diabetes mellitus. This study has shown that PEGylated SLNs represent a promising approach for improving the duration and delivery of metformin for effective treatment of diabetes, thus necessitating further development of the formulation.

Declarations

Author contribution statement

Kenechukwu, Franklin Chimaobi: Conceived and designed the experiments; Analyzed and interpreted the data; Contributed reagents, materials, analysis tools or data; Wrote the paper.

Nnamani, Daniel Okwudili; Duhu, Judith Chekwube: Performed the experiments; Analyzed and interpreted the data; Wrote the paper.

Nmesirionye, Bright Ugochukwu: Analyzed and interpreted the data; Wrote the paper.

Momoh, Mumuni Audu; Akpa, Paul Achile; Attama, Anthony Amaechi: Contributed reagents, materials, analysis tools or data; Wrote the paper.

Funding statement

This work was supported by Tertiary Education Trust Fund (TETFund) (Grant no. TETFUND/DR&D/CE/NRF/2019/STI/46/) by Government of Nigeria.

Data availability statement

The authors are unable or have chosen not to specify which data has been used.

Declaration of interests statement

The authors declare no conflict of interest.

Additional information

No additional information is available for this paper.

Acknowledgements

Dr. Franklin C. Kenechukwu wishes to acknowledge Phospholipid GmbH, Köln, Germany for generous provision of Phospholipon® 90H (P90H), Ph. Eur. Carl Roth GmbH + Co. KG Karlsruhe, Germany for the king gift of polyethylene glycol 4000 (PEG 4000) and beeswax as well as Gattefossé, Saint – Priest Cedex, France for supplying Capryol-PGE 860 used in this research.

References

[1] American Diabetes Association, Diagnosis and classification of diabetes mellitus, Diabetes Care 37 (Supplement_1) (2014 Jan 1) S81–90.
[2] H. Nasri, M. Rafieian-Kopaei, Metformin: current knowledge, J. Res. Med. Sci. Off. J. Isfahan Univ. Med. Sci. 19 (7) (2014 Jul) 658–664.
[3] K. Suvi, M. Belma, S. Pouya, S. Paraskevi (Eds.), IDF Diabetes Atlas, ninth ed., International Diabestes Federation, 2019. Available from: www.diabetesatlas.org.
[4] E. Sanchez-Rangel, S.E. Inzucchi, Metformin: clinical use in type 2 diabetes, Diabetologia 60 (9) (2017 Sep) 1586–1593.
[5] M. Momoh, F. Kenechukwu, A. Attama, Formulation and evaluation of novel solid lipid microparticles as a sustained release system for the delivery of metformin hydrochloride, Drug Deliv 20 (3-4) (2013) 102–111.
[6] N.T. Shurrab, E.-S.A. Arafa, Metformin: a review of its therapeutic efficacy and adverse effects, Obes. Med. 17 (2020 Mar) 100186.
[7] Y.-W. Wang, S.-J. He, X. Feng, J. Cheng, Y.-T. Luo, L. Tian, et al., Metformin: a review of its potential indications, Drug Des. Dev. Ther. 11 (2017 Aug) 2421–2429.
[8] Y. Chen, X. Shan, C. Luo, Z. He, Emerging nanoparticulate drug delivery systems of metformin, J. Pharm. Investig. 50 (3) (2020 May) 219–230.
[9] R. Muller, K. Mader, S. Gohla, Solid lipid nanoparticles (SLN) for controlled drug delivery – a review of the state of the art, Eur. J. Pharm. Biopharm. 50 (1) (2000 Jul 3) 161–177.
[10] S.K. Shukla, N.S. Kulkarni, A. Chan, V. Parvathaneni, P. Farrales, A. Muth, et al., Metformin-encapsulated liposome delivery system: an effective treatment approach against breast cancer, Pharmaceutics 11 (11) (2019 Oct 28). Available from: http://www.ncbi.nlm.nih.gov/pmc/articles/PMC6920889/.
[11] M. Momoh, M. Adedokun, M. Adikwu, F. Kenechukwu, E. Ibezim, E. Ugwoke, Design, characterization and evaluation of PEGylated-mucin for oral delivery of metformin hydrochloride, Afr. J. Pharm. Pharmacol. 7 (7) (2013) 347–355.
[12] S. Kumar, G. Bhanjana, R.K. Verma, D. Dhingra, N. Dilbaghi, K.-H. Kim, Metformin-loaded alginate nanoparticles as an effective antidiabetic agent for controlled drug release, J. Pharm. Pharmacol. 69 (2) (2017 Jan 19) 143–150.
[13] S. Bhujbal, A.K. Dash, Metformin-loaded hyaluronic acid nanostructure for oral delivery, AAPS PharmSciTech 19 (6) (2018 Aug) 2543–2553.
[14] C. Santhosh, K. Deivasigamani, R. Venkata, Enhanced effects of metformin loaded chitoson nanoparticles in L6 myotubes: in vitro, Der Pharm. Lett. 9 (7) (2017) 48–63.
[15] A.K. Sahu, A. Verma, Development and statistical optimization of chitosan and eudragit based gastroretentive controlled release multiparticulate system for bioavailability enhancement of metformin HCl, J. Pharm. Investig. 46 (3) (2016 Jun) 239–252.
[16] A.A. Hasan, H. Madkor, S. Wageh, Formulation and evaluation of metformin hydrochloride-loaded niosomes as controlled release drug delivery system, Drug Deliv 20 (3-4) (2013 Apr) 120–126.
[17] S.S. Rostamkalaei, J. Akbari, M. Saeedi, K. Morteza-Semnani, A. Nokhodchi, Topical gel of Metformin solid lipid nanoparticles: a hopeful promise as a dermal delivery system, Colloids Surf. B Biointerfaces 175 (2019 Mar) 150–157.
[18] R. Sharma, N. Sharma, S. Rana, H. Shivkumar, Solid lipid nanoparticles as a carrier of metformin for transdermal delivery, Int. J. Drug Deliv. 5 (2013) 137–145.
[19] P. Adhikari, P. Pal, A.K. Das, S. Ray, A. Bhattacharjee, B. Mazumder, Nano lipid-drug conjugate: an integrated review, Int. J. Pharm. 529 (1-2) (2017 Aug) 629–641.
[20] A. Attama, M. Momoh, P. Builders, Lipid nanoparticulate drug delivery systems: a revolution in dosage form design and development, in: A.D. Sezer (Ed.), Recent Advances in Novel Drug Carrier Systems, InTech, Rijeka,Croatia, 2012 [cited 2021 May 28]. p. 107–40. Available from: http://www.intechopen.com/books/recent-ad

vances-in-novel-drug-carrier-systems/lipid-nanoparticulate-drug-delivery-systems-a-revolution-in-dosage-form-design-and-development.
[21] S.A. Chime, I.V. Onyishi, Lipid-based drug delivery systems (LDDS): recent advances and applications of lipids in drug delivery, Afr. J. Pharm. Pharmacol. 7 (48) (2013) 3034–3059.
[22] J. Pardeike, A. Hommoss, Müller Rh, Lipid nanoparticles (SLN, NLC) in cosmetic and pharmaceutical dermal products, Int. J. Pharm. 366 (1-2) (2008 Oct 17) 170–184.
[23] A. Kovacevic, S. Savic, G. Vuleta, R.H. Müller, C.M. Keck, Polyhydroxy surfactants for the formulation of lipid nanoparticles (SLN and NLC): effects on size, physical stability and particle matrix structure, Int. J. Pharm. 406 (1-2) (2011) 163–172.
[24] K.L. Guimarães, M.I. Ré, Lipid nanoparticles as carriers for cosmetic ingredients: the first (SLN) and the second generation (NLC), in: Nanocosmetics and Nanomedicines, Springer, Berlin, Heidelberg, 2011 [cited 2021 May 31]. p. 101–22. Available from: https://link.springer.com/chapter/10.1007/978-3-642-19792-5_5.
[25] V.J. Lingayat, N.S. Zarekar, R.S. Shendge, Solid lipid nanoparticles: a review, Nanosci. Nanotechnol. Res. 4 (2) (2017) 67–72.
[26] E.B. Souto, I. Baldim, W.P. Oliveira, R. Rao, N. Yadav, F.M. Gama, et al., SLN and NLC for topical, dermal, and transdermal drug delivery, Expet Opin. Drug Deliv. 17 (3) (2020 Mar 3) 357–377.
[27] R. Shah, D. Eldridge, E. Palombo, I. Harding, Lipid Nanoparticles: Production, Characterization and Stability, Springer International Publishing, Cham, 2015 (SpringerBriefs in Pharmaceutical Science & Drug Development). Available from: http://link.springer.com/10.1007/978-3-319-10711-0.
[28] V. Mishra, K. Bansal, A. Verma, N. Yadav, S. Thakur, K. Sudhakar, et al., Solid lipid nanoparticles: emerging colloidal nano drug delivery systems, Pharmaceutics 10 (4) (2018 Oct 18) 191.
[29] A. Reddy, S. Parthiban, A. Vikneswari, G. Senthilkumar, A modern review on solid lipid nanoparticles as novel controlled drug delivery system, Int. J. Res. Pharm. Nano Sci. 3 (4) (2014) 313–325.
[30] S.K. Basha, R. Dhandayuthabani, M.S. Muzammil, V.S. Kumari, Solid lipid nanoparticles for oral drug delivery, Mater. Today Proc. 36 (2021) 313–324.
[31] F.C. Kenechukwu, A.A. Attama, E.C. Ibezim, P.O. Nnamani, C.E. Umeyor, E.M. Uronnachi, et al., Novel intravaginal drug delivery system based on molecularly PEGylated lipid matrices for improved antifungal activity of miconazole nitrate, BioMed Res. Int. 2018 (2018 Jun 6) 1–18.
[32] R. van der Meel, E. Sulheim, Y. Shi, F. Kiessling, W.J.M. Mulder, T. Lammers, Smart cancer nanomedicine, Nat. Nanotechnol. 14 (11) (2019 Nov) 1007–1017.
[33] Q. Chen, G. Liu, S. Liu, H. Su, Y. Wang, J. Li, et al., Remodeling the tumor microenvironment with emerging nanotherapeutics, Trends Pharmacol. Sci. 39 (1) (2018 Jan) 59–74.
[34] C. Luo, J. Sun, Y. Du, Z. He, Emerging integrated nanohybrid drug delivery systems to facilitate the intravenous-to-oral switch in cancer chemotherapy, J. Contr. Release 176 (2014 Feb) 94–103.
[35] O.K. Nag, V. Awasthi, Surface engineering of liposomes for stealth behavior, Pharmaceutics 5 (4) (2013 Dec) 542–569.
[36] J.S. Suk, Q. Xu, N. Kim, J. Hanes, L.M. Ensign, PEGylation as a strategy for improving nanoparticle-based drug and gene delivery, Adv. Drug Deliv. Rev. 99 (2016 Apr 1) 28–51.
[37] Y. Dai, H. Xing, F. Song, Y. Yang, Z. Qiu, X. Lu, et al., Biotin-conjugated multilayer poly [D,L-lactide-co-glycolide]-Lecithin-Polyethylene glycol nanoparticles for targeted delivery of doxorubicin, J. Pharmacol. Sci. 105 (9) (2016 Sep 1) 2949–2958.
[38] M. Ways Tm, W.M. Lau, V.V. Khutoryanskiy, Chitosan and its derivatives for application in mucoadhesive drug delivery systems, Polymers 10 (3) (2018 Mar) 267.
[39] A. Chakraborty, A. Bhattacharjee, D. Dutta, S. Dutta, G. Mukhopadhyay, A review on some formulation strategies to improve the bioavailability of drugs with low permeability and high solubility (BCS III), Int. J. Pharm. Eng. 4 (1) (2016) 683–690.
[40] F.C. Kenechukwu, E.C. Ibezim, A.A. Attama, M.A. Momoh, J.D.N. Ogbonna, P.O. Nnamani, et al., Preliminary spectroscopic characterization of PEGylated mucin, a novel polymeric drug delivery system, Afr. J. Biotechnol. 12 (47) (2013) 6661–6671.
[41] A. Attama, C. Okafor, P. Builders, O. Okorie, Formulation and *in vitro* evaluation of a PEGylated microscopic lipospheres delivery system for ceftriaxone sodium, Drug Deliv 16 (8) (2009) 448–457.
[42] M.A. Momoh, F.C. Kenechukwu, A.A. Attama, Formulation and evaluation of novel solid lipid microparticles as a sustained release system for the delivery of metformin hydrochloride, Drug Deliv 20 (3 – 4) (2013) 102–111.
[43] Phosphate Buffer (pH 5.8 to 7.4) Recipe and Preparation, AAT Bioquest, 2018 [cited 2021 Jun 2]. Available from: https://www.aatbio.com/resources/buffer-preparations-and-recipes/phosphate-buffer-ph-5.8-to-7.4.
[44] P. Ghasemiyeh, S. Mohammadi-Samani, Solid lipid nanoparticles and nanostructured lipid carriers as novel drug delivery systems: applications, advantages and disadvantages, Res. Pharm. Sci. 13 (4) (2018) 288–303.
[45] F. Kenechukwu, M. Momoh, C. Umeyor, E. Uronnachi, A. Attama, Investigation of novel solid lipid microparticles based on homolipids from *Bos indicus* for the delivery of gentamicin, Int. J. Pharm. Investig. 6 (1) (2016) 32–38.
[46] M. Uner, Preparation, characterization and physico-chemical properties of Solid Lipid Nanoparticles (SLN) and Nanostructured Lipid Carriers (NLC): their benefits as colloidal drug carrier systems, Pharmazie 61 (2005) 375–386.
[47] J.N. Reginald-Opara, A. Attama, K. Ofokansi, C. Umeyor, F. Kenechukwu, Molecular interaction between glimepiride and Soluplus ® -PEG 4000 hybrid based solid dispersions: characterisation and anti-diabetic studies, Int. J. Pharm. 496 (2) (2015 Dec) 741–750.
[48] F.C. Kenechukwu, M.A. Momoh, P.O. Nnamani, C.E. Umeyor, E.M. Uronnachi, M.L. Dias, E.C. Ibezim, A.A. Attama, Dual-responsive micellar microgels matrixed with surface-engineered lipids: a new approach for controlled vaginal drug delivery, J. Pharm. Innov. 2021 (2021). Eraly online:1-19.
[49] S. Tsutsumi, M. Iida, N. Tada, T. Kojima, Y. Ikeda, T. Moriwaki, et al., Characterization and evaluation of miconazole salts and cocrystals for improved physicochemical properties, Int. J. Pharm. 421 (2) (2011 Dec) 230–236.
[50] S. Javidfar, Y. Pilehvar-Soltanahmadi, R. Farajzadeh, J. Lotfi-Attari, V. Shafiei-Irannejad, M. Hashemi, et al., The inhibitory effects of nano-encapsulated metformin on growth and hTERT expression in breast cancer cells, J. Drug Deliv. Sci. Technol. 43 (2018) 19–26.
[51] V.K. Kamboj, P.K. Verma, Preparation and characterization of metformin loaded Stearic Acid coupled F127 Nanoparticles, Asian J. Pharmaceut. Clin. Res. 11 (8) (2018) 212–217.
[52] G. Sharma, A.K. Parchur, J.M. Jagtap, C.P. Hansen, A. Joshi, Hybrid nanostructures in targeted drug delivery, in: Hybrid Nanostructures for Cancer Theranostics, Elsevier, 2019, pp. 139–158. Available from: https://linkinghub.elsevier.com/retrieve/pii/B9780128139066000081.
[53] K.J. Wadher, R.B. Kakde, M.J. Umekar, Development of a sustained-release tablet of metformin hydrochloride containing hydrophilic eudragit and ethyl cellulose polymer, Int. J. Compr. Pharm. 2 (5) (2011) 1–6.
[54] N.C. Ngwuluka, D.J. Kotak, P.V. Devarajan, Design and characterization of metformin-loaded solid lipid nanoparticles for colon cancer, AAPS PharmSciTech 18 (2) (2017 Feb) 358–368.
[55] Q. Xu, T. Zhu, C. Yi, Q. Shen, Characterization and evaluation of metformin-loaded solid lipid nanoparticles for celluar and mitochondrial uptake, Drug Dev. Ind. Pharm. 42 (5) (2016 May 3) 701–706.
[56] J. Siepmann, N. Peppas, Higuchi equation: derivation, applications, use and misuse, Int. J. Pharm. 418 (2011) 6–12.
[57] C. Santhosh, K. Deivasigamani, V. Galeda, Development and characterization of metformin loaded pectin nanoparticles for T2 diabetes mellitus, Pharm. Nanotechnol. 6 (2018) 253–263.
[58] I. Permanadewi, A. Kumoro, D. Wardhani, N. Aryanti, Modelling of controlled drug release in gastrointestinal tract simulation, J. Phys. Conf. Ser. 1295 (2019) 1–8.
[59] I.Y. Wu, S. Bala, N. Škalko-Basnet, M.P. di Cagno, Interpreting non-linear drug diffusion data: utilizing Korsmeyer-Peppas model to study drug release from liposomes, Eur. J. Pharmaceut. Sci. 138 (2019 Oct) 105026.
[60] A. Olejnik, A. Kapuscinska, G. Schroeder, I. Nowak, Physico-chemical characterization of formulations containing endomorphin-2 derivatives, Amino Acids 49 (10) (2017 Oct) 1719–1731.
[61] C.J.H. Porter, N.L. Trevaskis, W.N. Charman, Lipids and lipid-based formulations: optimizing the oral delivery of lipophilic drugs, Nat. Rev. Drug Discov. 6 (3) (2007 Mar) 231–248.
[62] E.C. Ossai, A.C. Madueke, B.E. Amadi, M.O. Ogugofor, M.A. Momoh, C.O.R. Okpala, et al., Potential enhancement of metformin hydrochloride in lipid vesicles targeting therapeutic efficacy in diabetic treatment, Int. J. Mol. Sci. 22 (2852) (2021) 1–16.